Journal of the Air & Waste Management Association

ISSN: 1096-2247 (Print) 2162-2906 (Online) Journal homepage: https://www.tandfonline.com/loi/uawm20

Measurement of fine particulate matter water-soluble inorganic species and precursor gases in the Alberta Oil Sands Region using an improved semicontinuous monitor

Yu-Mei Hsu & Thomas A. Clair

To cite this article: Yu-Mei Hsu & Thomas A. Clair (2015) Measurement of fine particulate matter water-soluble inorganic species and precursor gases in the Alberta Oil Sands Region using an improved semicontinuous monitor, Journal of the Air & Waste Management Association, 65:4, 423-435, DOI: 10.1080/10962247.2014.1001088

To link to this article: https://doi.org/10.1080/10962247.2014.1001088

TECHNICAL PAPER

Measurement of fine particulate matter water-soluble inorganic species and precursor gases in the Alberta Oil Sands Region using an improved semicontinuous monitor

Yu-Mei Hsu* and Thomas A. Clair

Wood Buffalo Environmental Association, Fort McMurray, Alberta, Canada

**Please address correspondence to: Yu-Mei Hsu, Wood Buffalo Environmental Association, No. 100–330 Thickwood Boulevard, Fort McMurray, Alberta, Canada, T9K 1Y1; e-mail: yhsu@wbea.org*

The ambient ion monitor–ion chromatography (AIM-IC) system, which provides hourly measurements of the main chemical components of $PM_{2.5}$ (particulate matter with an aerodynamic diameter <2.5 μm) and its precursor gases, was evaluated and deployed from May to July 2011 and April to December 2013 in the Athabasca Oil Sands Region (AOSR) of northeastern Alberta, Canada. The collection efficiencies for the gas-phase SO_2 and HNO_3 using the cellulose membrane were 96% and 100%, respectively, and the collection efficiency of NH_3 using the nylon membrane was 100%. The AIM-IC was compared with a collocated annular denuder sampling system (ADSS) and a Federal Reference Method (FRM) Partisol $PM_{2.5}$ sampler. The correlation coefficients of SO_4^{2-} concentrations between the AIM-IC and ADSS and between the AIM-IC and the Partisol $PM_{2.5}$ sampler were 0.98 and 0.95, respectively. The comparisons also showed no statistically significant difference between the measurement sets, suggesting that the AIM-IC measurements of the $PM_{2.5}$ chemical composition are comparable to the ADSS and Partisol $PM_{2.5}$ methods. NH_3 concentration in the summer (mean ± standard deviation, 1.9 ± 0.7 μg m^{-3}) was higher than in the winter (1.3 ± 0.9 μg m^{-3}). HNO_3 and NO_3^- concentrations were generally low in the AOSR, and especially in the winter months. NH_4^+ (0.94 ± 0.96 μg m^{-3}) and SO_4^{2-} (0.58 ± 0.93 μg m^{-3}) were the major ionic species of $PM_{2.5}$. Direct SO_2 emissions from oil sands processing operations influenced ambient particulate NH_4^+ and SO_4^{2-} values, with hourly concentrations of NH_4^+ and SO_4^{2-} measured downwind (~30 km away from the stack) at 10 and 28 μg m^{-3}. During the regional forest fire event in 2011, high concentrations of NO_3^-, NH_4^+, HNO_3, NH_3, and $PM_{2.5}$ were observed and the corresponding maximum hourly concentrations were 31, 15, 9.6, 89, and >450 (the upper limit of $PM_{2.5}$ measurement) μg m^{-3}, suggesting the formation of NH_4NO_3.

Implications: The AOSR in Canada is one of the most scrutinized industrial regions in the developed world due to the extent of oil extraction activities. Because of this, it is important to accurately assess the effect of these operations on regional air quality. In this study, we compare a new analytical approach, AIM-IC, with more standard analytical approaches to understand how local anthropogenic and nonanthropogenic sources (e.g., forest fires) impact regional air quality. With this approach, we also better characterize $PM_{2.5}$ composition and its precursor gases to understand secondary aerosol formation mechanisms and to better identify possible control techniques if needed.

Introduction

The Athabasca Oil Sands Region (AOSR) in the northeastern part of Alberta, Canada, contains some of the largest oil sands deposits in the world, with production expected to increase from 1.9 million barrels per day in 2012 to 3.8 million barrels per day in 2022 (Stringham, 2012). In recent years, oil sands development has attracted global attention, in part due to environmental concerns such as acidification and eutrophication. The Wood Buffalo Environmental Association (WBEA; www.wbea.org) has monitored the air quality in the AOSR since 1998, using continuous and time-integrated methods. Overall, in 2012, no exceedance for the Alberta Ambient Air Quality Objectives occurred for sulfur dioxide (SO_2), nitrogen dioxide (NO_2), and ammonia (NH_3) concentrations; 1 for ozone (O_3); 170 for hydrogen sulfide/total reduced sulfur; and 62 for $PM_{2.5}$ (particulate matter with an aerodynamic diameter <2.5 μm) (Percy, 2013). The current Canadian Ambient Air Quality Standard (CAAQS) for $PM_{2.5}$ is 30 μg m^{-3} for 24-hr average, but this is changing in 2015 to 10 μg m^{-3} for the annual average and 28 μg m^{-3} for the 24-hr average (https://www.ec.gc.ca/), so that considering the new objectives, it is more important to understand $PM_{2.5}$ characterization and its formation mechanisms.

The major air pollutants emitted from oil sands processing are sulfur and nitrogen oxides, particulate matter, and volatile organic compounds (Gosselin et al., 2010; Davies et al., 2012).

Journal of the Air & Waste Management Association, 65(4):423–435, 2015. ISSN: 1096-2247 print
DOI: 10.1080/10962247.2014.1001088 Submitted June 3, 2014; final version submitted December 16, 2014; accepted December 16, 2014.
Color versions of one or more of the figures in the article can be found online at www.tandfonline.com/uawm.

One of the methods WBEA had been using to measure regional atmospheric contaminants was an annular denuder sampling system (ADSS). This approach measures the concentrations of gas-phase species, including SO_2, nitric acid (HNO_3), NH_3, and fine particulate matter ($PM_{2.5}$) species, including sulfate (SO_4^{2-}), nitrate (NO_3^-), and ammonium (NH_4^+), primarily to investigate the abundance of ambient N species in order to assess potential eutrophication of terrestrial and aquatic ecosystems. Investigating NH_3 and NH_4^+ partitioning in the AOSR is important, as gas-phase NH_3 and particulate-phase NH_4^+ are removed by dry deposition at significantly different rates. Gas-phase NH_3 has about an order of magnitude greater deposition velocity than the particulate NH_4^+ (Seinfeld and Pandis, 2006).

The generally low concentrations of these chemical species in the AOSR requires 24-hr sampling to obtain sufficient amounts of the chemicals to be measured using current approaches. The ADSS sampling, therefore, analyzed samples collected over 24 hr every 6 days based on the Canadian National Air Pollution Surveillance (NAPS) network schedule (http://www.ec.gc.ca/rnspa-naps/). The ADSS monitoring approach in the context of the AOSR has a number of disadvantages, which include (1) it is labor-intensive, as the denuder requires precoating; (2) samples collected required an extraction process with associated potential for introduced biases, e.g., incomplete recovery of a sample; and (3) 24-hr sampling intervals result in poor temporal resolution and did not provide information on the diurnal variability of trace pollutants.

To provide lower compound detection levels and better sample time resolution, WBEA deployed a new semicontinuous instrument, an ambient ion monitor–ion chromatograph (AIM-IC). This instrument measures gas-phase SO_2, HNO_3, NH_3, and HCl, as well as water-soluble $PM_{2.5}$ compositions (SO_4^{2-}, NO_3^-, and NH_4^+). Simultaneous gas- and particulate-phase measurements of these compounds were performed at a 1-hr time resolution. The data generated provided near-real-time information on important pollutant concentrations that could be used to better understand the atmospheric chemistry in the AOSR. This in turn allows the impacts of oil sands operations on regional air quality to be better understood.

A similar analyzer to the AIM-IC unit that is used by WBEA is the monitoring for aerosols and gases (MARGA) instrument (Makkonen et al., 2012). The AIM-IC and MARGA have been successfully used in several large-scale studies: in Shanghai and Beijing, China, for $PM_{2.5}$ sulfate and nitrate characterization (Wu and Wang, 2007; Nie et al., 2010; Du et al., 2011); in Lanzhou City, China, for the formation mechanism of secondary aerosol pollution (Fan et al., 2014); in Jinan, China, for $PM_{2.5}$ temporal variations and source apportionments (Gao et al., 2011); in Singapore for inorganic compounds in aerosols and gases characterization (Khezri et al., 2013); in southwestern Ontario, Canada, for studying transboundary air pollution (Ellis et al., 2011); in San Joaquin Valley, California, USA, for gas-particle partitioning study during the California Nexus (CalNex) 2010 campaign (Ahlm et al., 2012); and in India for $PM_{2.5}$ water-soluble ionic species characterization (Sudheer et al., 2014). However, the approach has never been used to better understand atmospheric N dynamics in a focused industrial setting (bitumen upgrading) in a region with extremely cold winter conditions.

The region is also subjected to episodes of large-scale forest fires, which have important effects to regional air quality. During the wild fires, $PM_{2.5}$ concentrations often exceeded the ambient air quality objective and the hourly concentration could be higher than the 1000 μg m^{-3}. The exposure to high $PM_{2.5}$ concentration has been associated with many adverse health effects, including asthma, acute respiratory symptoms, chronic bronchitis, and declined lung function (Upadhyay et al., 2014), as well as the impact to ecosystem. The $PM_{2.5}$ chemical composition characterization during the wild fire is important.

The objectives of this study were therefore (1) to evaluate the performance characteristics of WBEA's AIM-IC under the unique climate and industrial conditions of the AOSR; (2) to compare results with two standard methods that are widely used, the ADSS and the Federal Reference Method (FRM) Partisol $PM_{2.5}$ sampler; (3) if validated by the methods of comparison, to use the AIM-IC to quantify the concentrations of SO_2, HNO_3, NH_3, SO_4^{2-}, NO_3^-, and NH_4^+ in the AOSR and compare the values with those measured elsewhere to provide an assessment of the relative scale of the air pollution problem in the AOSR; and (4) to identify the major $PM_{2.5}$ formation mechanisms (inorganic species) with the local emission sources (i.e., oil sands operation and forest fire) during episodes (e.g., exceedance).

Methods

AIM-IC

The AIM-IC deployed in the AOSR consists of the ambient ion monitor (model AIM 9000D; University Research Glassware Corp., Chapel Hill, NC, USA) for collection of ambient gases and particles into aqueous solution, and two ion chromatography (IC) systems (model ICS-2000; Dionex Corp., Sunnyvale, CA, USA) for the simultaneous analyses of anions and cations in the collected samples. The ambient air enters the AIM-IC through a Teflon-coated total suspended particulate (TSP) inlet. A coupler-impactor (URG-3000-30P; University Research Glassware) with elutriator inlet (URG-2000-30KN2; University Research Glassware) is then used to remove particles with an aerodynamic diameter larger than 2.5 μm (Figure 1).

The air containing a mixture of $PM_{2.5}$ and gases is passed through a parallel-plate wet denuder (PPWD) where soluble gases (e.g., SO_2, HNO_3, and NH_3) are collected in 5 mM solution of H_2O_2 in ultrapure deionized water (18.2 MΩ). H_2O_2 is used to oxidize the sparingly soluble SO_2 to SO_4^{2-} and improve collection. The membranes used in the PPWD are a cellulose membrane for acidic gas collection/analysis and a nylon membrane for NH_3 collection/analysis. The $PM_{2.5}$ next enters a particle super saturation chamber (PSSC) where steam is used to dissolve water-soluble compounds, including, but not limited to, SO_4^{2-}, NO_3^-, and NH_4^+.

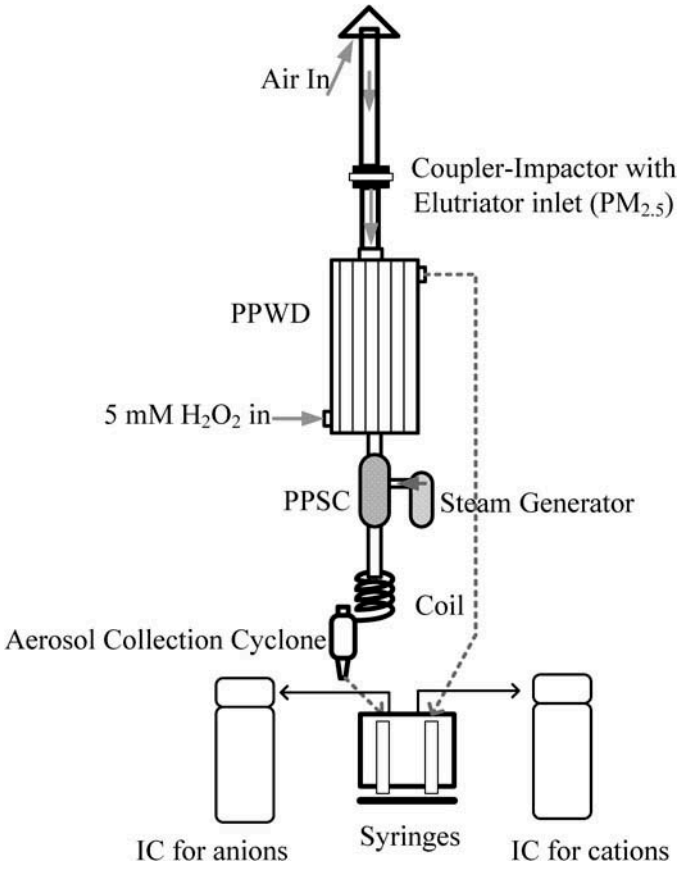

Figure 1. Schematic figure of AIM-IC. PPWD = parallel-plate wet denuder; PPSC = particle supersaturation chamber.

The dissolved water-soluble compounds in particulate phase are collected in an aerosol collection cyclone. The resultant gas and particle samples are stored in glass syringes for analysis. After 1 hr of sampling, the samples are injected onto two IC systems for simultaneous anion and cation analyses. Quarterly calibration and monthly checks of the AIM-IC are performed by offline injections of aqueous standards into the IC systems. From the signals acquired via the two IC systems, the ambient concentrations of gases and particles are calculated and reported as per Markovic et al. (2012). The detection limits (3 × standard deviation of seven measurements) of AIM-IC are 89, 93, and 43 ng m^{-3} for NH_4^+, NO_3^-, and SO_4^{2-}; 84, 95, and 14 ng m^{-3} for NH_3, HNO_3, and SO_2.

Laboratory evaluation of the AIM-IC system

The AIM-IC system evaluation was performed for SO_2, HNO_3, and NH_3, which are usually the most abundant water-soluble trace gas precursors of $PM_{2.5}$. A Dynacalibrator calibration gas generator (model 450; VICI Metronics, Poulsbo, WA, USA) with Dynacal permeation tubes (VICI Metronics) was used in conjunction with zero-air cylinders to generate known concentrations of SO_2, HNO_3, and NH_3 gas standards. These standards were used to determine the collection efficiency (eq 1) and the response time of the AIM-IC in the laboratory.

$$\text{Collection efficiency (\%)} = [\text{Gas}]_{\text{PPWD}} \times 100\% / \left([\text{Gas}]_{\text{PPWD}} + [\text{Particle}]_{\text{PSSC}}\right) \quad (1)$$

where $[\text{Gas}]_{\text{PPWD}}$ is the amount measured in gaseous phase collected by PPWD (μg) and $[\text{Particle}]_{\text{PSSC}}$ is the amount measured in particulate phase collected by PSSC (μg).

Both cellulose and nylon membranes were evaluated for use in the PPWD. The permeation rates (certified by VICI Metronics) of SO_2, HNO_3, and NH_3 (at 30 °C) were 7.91, 3.88, and 0.95 μg hr^{-1}, respectively. The permeation rates were then divided by the flow rate of zero air to produce the introduced concentrations. The concentrations introduced to the AIM-IC were (1) 22.0, 33.0, and 43.9 μg m^{-3} for SO_2; (2) 10.8, 16.2, and 21.6 μg m^{-3} for HNO_3; (3) 2.6, 4.0, and 5.3 μg m^{-3} for NH_3. Blanks were run by flowing pure zero-air gas (Praxair Canada Inc., Mississauga, ON, Canada) from the cylinders to the Dynacalibrator calibration gas generator and then into the inlet of the AIM-IC system. All tubing was made of Teflon to minimize losses of "sticky" gases such as SO_2, HNO_3, and NH_3.

Field comparison of the gas- and particle-phase measurements of the WBEA's AIM-IC

A commercial, Federal Equivalent Method (FEM) real-time continuous SO_2 monitor (model 43C; Thermo Scientific, Franklin, MA, USA) was collocated with the AIM-IC for an intercomparison and field validation of the SO_2 measurements acquired via the AIM-IC. The SO_2 monitor underwent daily zero/span and monthly calibrations in the field. As other precursor gas monitors, i.e., HNO_3 and NH_3, were not available, the validity of the WBEA's AIM-IC system for ambient measurements of HNO_3 and NH_3 was assessed based on the results of the SO_2 intercomparison.

Ambient measurements of the $PM_{2.5}$ composition with an ADSS (University Research Glass) with a Teflon membrane filter were used to assess the accuracy of the AIM-IC by comparison under field conditions in 2011. The ADSS has been widely used for simultaneous monitoring of gas- and particulate-phase inorganic species (Ferm and Sjodin, 1985; Brauer et al., 1989; Febo, Perrino, and Cortiello, 1993). The ADSS, consisting of annular denuders and a filter pack, minimizes the interactions of gases and particles by using the denuder to remove the gases of interest (Harrison and Kitto, 1990). The U.S. Environmental Protection Agency's (EPA) FRM $PM_{2.5}$ sampler (Partisol 2000-FRM; Thermo Scientific) with Teflon membrane filter was collocated with the AIM-IC for particulate-phase intercomparison from 2012 to 2013.

Tapered element oscillating microbalance (TEOM) monitor (model 1400A; Rupprecht and Patashnick Co., Albany, NY, USA) in May 2011 and EPA FEM synchronized hybrid ambient real-time particulate (SHARP) monitor (model 5030; Thermo Scientific) from June to July 2011 were applied to monitor real-time $PM_{2.5}$ mass concentrations and an NH_3 monitor (Thermo Electron Corp., Franklin, MA, USA) was employed for real-time NH_3 concentration (for concentration higher than 5 ppb) at

WBEA's Bertha Ganter–Fort McKay Air Monitoring Station (AMS 1). An O_3 monitor (model 49C; Thermo Scientific), a NO_2 monitor (model 42C; Thermo Scientific), a SO_2 monitor (model 43C; Thermo Scientific), a pyranometer (model SP Lite; Kipp & Zonen B.V., Delft, The Netherlands), and a temperature probe (model HMP155; Vaisala, Louisville, CO, USA) were employed to monitor the hourly O_3, NO_2, and SO_2 concentrations, global solar radiation (GSR), and ambient temperature at WBEA's Athabasca Valley Station (AMS 7). All continuous monitors met the requirements of 1989 Alberta's Air Monitoring Directive. These instruments are commercially available and more details can be found at http://www.wbea.org/air-monitoring/standard-operating-procedures.

Sampling sites

The AIM-IC was located at WBEA's Bertha Ganter–Fort McKay Air Monitoring Station (AMS 1; 57.189°N, 111.640°W) from May 2011 to July 2011 and at the WBEA's Athabasca Valley Air Monitoring Station (AMS 7; 56.732°N, 111.390°W) from April 2013 to December 2013 (Figure 2). AMS 1 is located in the First Nation and Metis Community of Fort McKay, which is approximately within 15 km of four mining/upgrading operations. AMS 7, a community station, is located in downtown Fort McMurray, Alberta, 35 km to the south of these two oil sands operations. During the evaluation periods, the prevailing wind direction was from the south at AMS 1 and from the southeast at AMS 7.

Results and Discussion

System evaluation of the WBEA's AIM-IC for measurements of gases

The Dynacalibrator calibration gas generator was used to generate known concentrations of SO_2, HNO_3, and NH_3 gas standards, which were supplied to the AIM-IC with the cellulous and nylon membranes in the PPWD to examine the collection efficiencies and response times. Zero air as the method blank measurement and three various concentrations were introduced into the AIM-IC (Figure 3a, b, and c). At the first hour, only about 70%, 30%, and 56% of the delivered concentration of SO_2, HNO_3, and NH_3, respectively, were detected due to sample carryover of the method's blank solution, as a residual collected sample (aqueous solution) remains in the instrument tubing and the denuder (Markovic et al., 2012). With a decrease in known concentrations, the AIM-IC responded rapidly for all three species. When the zero air was reintroduced to the AIM-IC, the AIM-IC analyzed the residual sample in the tubing for approximately 1 hr and taking up to 3 hr to finally measure the delivered concentrations. It is important to note that the rapid concentration changes used in the AIM-IC evaluation are rarely observed under field conditions and that the instrument sample carryover should not present a serious measurement capability problem but needs to be recognized as a potential issue in certain circumstances. Although a known concentration of SO_2 was introduced to the

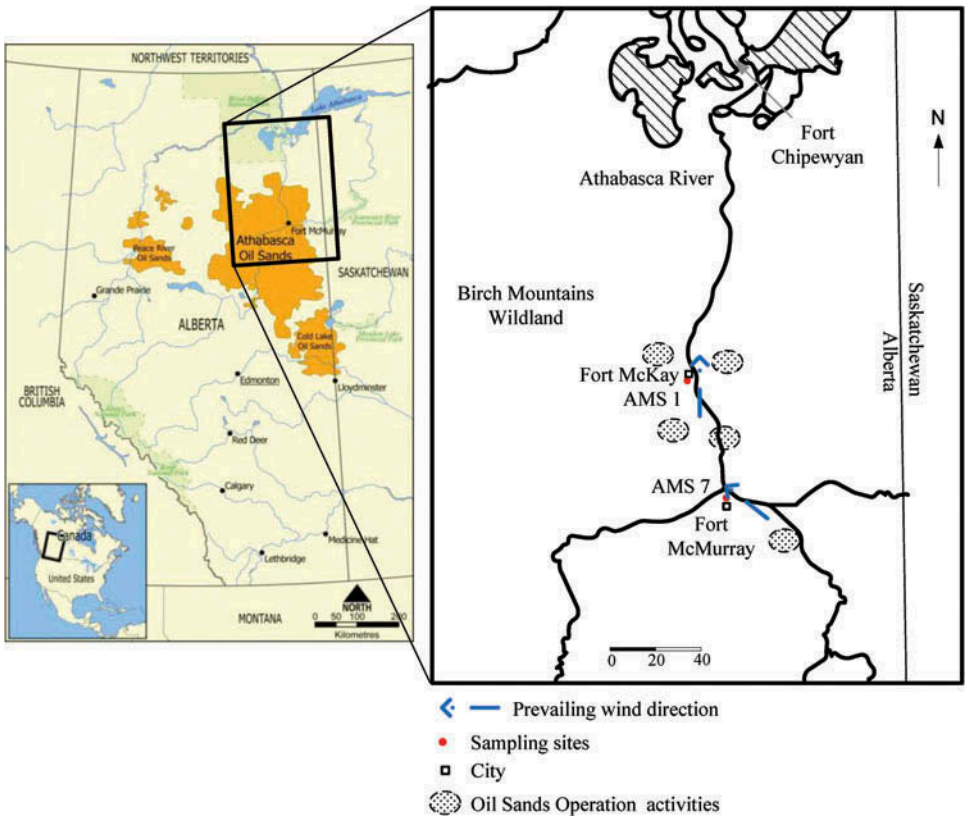

Figure 2. Map of sampling locations in Alberta, Canada (http://en.wikipedia.org/wiki/File:Athabasca_Oil_Sands_map.png).

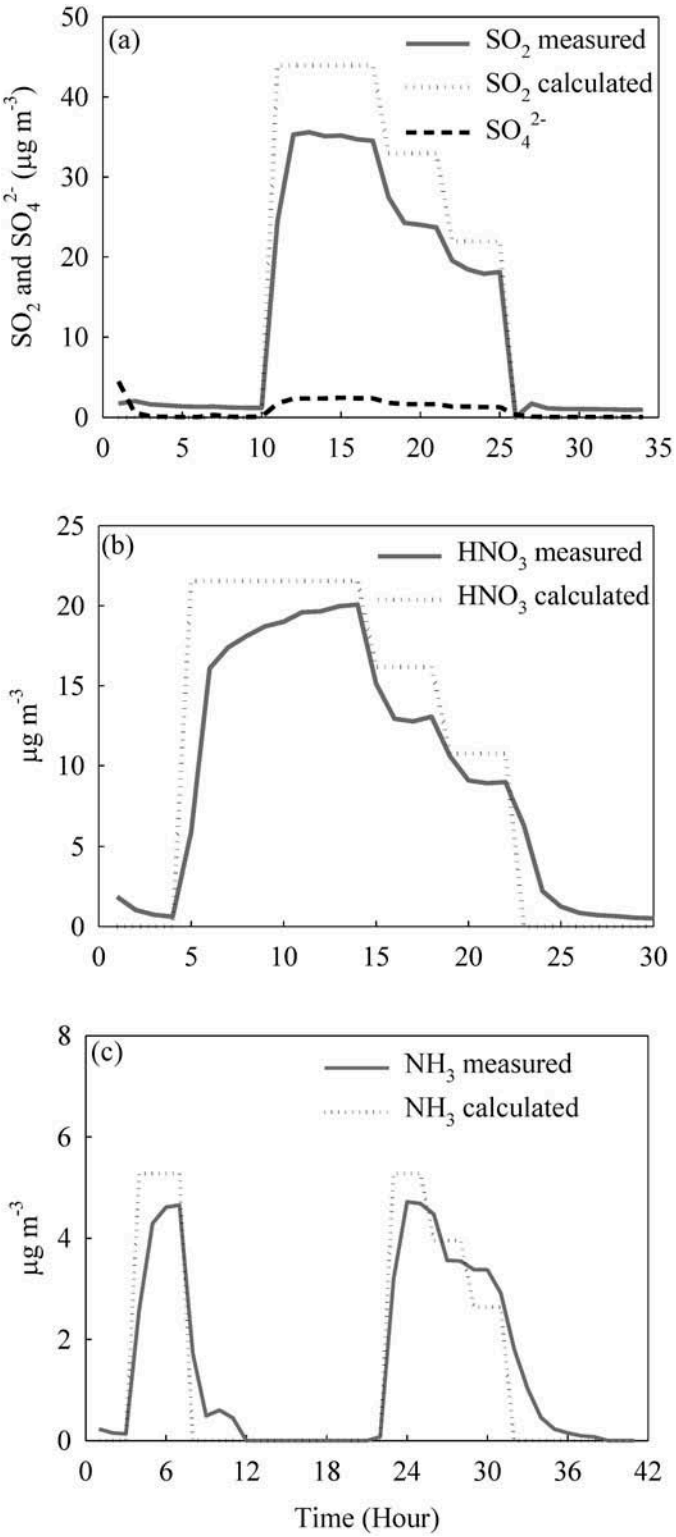

Figure 3. The time responses of the WBEA's AIM-IC system to known concentrations of (a) SO_2, (b) HNO_3, and (c) NH_3. The *y*-axes represent known concentrations of each chemical species delivered to the instrument from permeation sources each hour.

system, some SO_4^{2-} was also detected in particulate phase, indicating the penetration of SO_2 from the PPWD to the particle collector assembly. Hence, the SO_2 collection efficiency was determined to be 95.6 ± 0.12%. For HNO_3 and NH_3, no particulate nitrate and ammonium were observed and the collection efficiencies of HNO_3 and NH_3 were determined to be 100%. Sulfur dioxide is not as soluble as HNO_3, which would explain the lower collection efficiency for SO_2. The denuder membrane material (i.e., cellulose versus nylon) did not make a difference in collection efficiency nor response time for measurements of SO_2 and HNO_3, consistent with Markovic et al. (2012). The response testing of NH_3 using the cellulose membrane showed poor results. For all three species, the concentrations from theoretical calculation were higher than the concentrations measured by the AIM-IC. The biased low concentrations for SO_2, NH_3, and HNO_3 were also identified by Markovic et al. (2012). Possible reasons for the discrepancy are that the losses of SO_2, HNO_3, and NH_3 occurred before they reached the PPWD, or that the AIM-IC underestimated the SO_2, HNO_3, and NH_3 concentrations. Further validation needs to be carried out to investigate the potential cause(s) of this bias.

For SO_2 field validation, the real-time SO_2 monitor was collocated with the AIM-IC from April to December 2013 at AMS 7. The SO_2 intercomparison was reported every 3 months and the correlation coefficients for April to June, July to September, and October to December were 0.94 (number of samples = 1340), 0.82 (number of samples = 1748), and 0.71 (number of samples = 1955), respectively. The lowest detectable limit of the real-time SO_2 monitor was ~1 ppb. With the SO_2 calibration gas concentration of 1000 ppb, the lowest detectable limit could be around 2–3 ppb. Hence, the AIM-IC is the better tool in this range (low concentration). However, the SO_2 monitor could perform better in high SO_2 concentration range (>15 ppb) and the AIM-IC could have the SO_2 penetration problem when SO_2 concentration was high. The correlation coefficient dropping from 0.94 to 0.71 was because the SO_2 concentration distribution (maximum) varied in the three sampling periods. When SO_2 concentration was low (<1 ppb), the SO_2 monitor reported negative values sometimes. Those values would be replaced by zero, since the negative concentration was not possible, resulting in the lower correlation coefficient because of the shortcoming of SO_2 monitor in low SO_2 concentration range. High correlation coefficients of SO_2 concentrations from two measurements indicate method comparability and that the AIM-IC is suitable for the SO_2 monitoring.

Field evaluation of the WBEA's AIM-IC for aerosol composition measurements

An ADSS, a commonly used filter-based sampler for collection of gases and aerosols, was collocated with the AIM-IC at AMS 1 in 2011 for the evaluation of the aerosol composition measurements. Nonparametric measures were used for the statistical analysis because the results in this study were not normally distributed. The Spearman rank-order correlation coefficients from the intercomparison of particulate sulfate (number of samples = 33) and nitrate (number of samples = 29) measurements between the AIM-IC and the ADSS were 0.98 and 0.90 ($P < 0.01$), respectively (Figure 4). The *P* values of Mann-Whitney

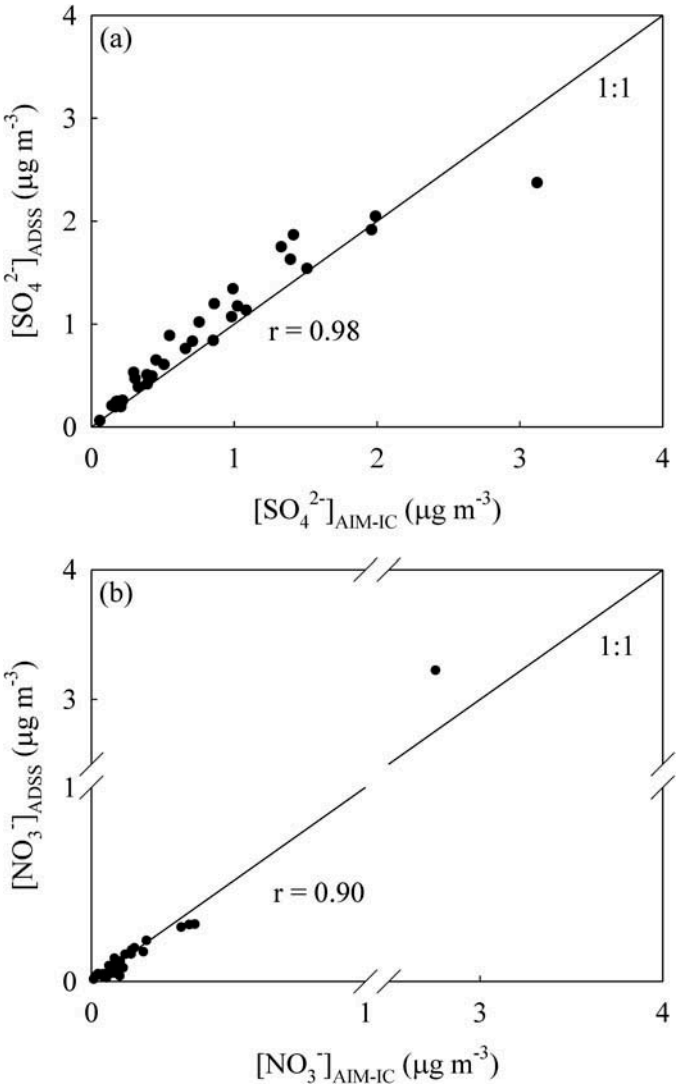

Figure 4. Intercomparison between AIM-IC and ADSS measurements of (a) sulfate and (b) nitrate (r is the Spearman rank-order correlation coefficient) at AMS 1.

rank-sum test (for learning if the concentrations from two measurements could be statistically significant difference) for both sulfate and nitrate were 0.36 and 0.35, respectively, indicating that there is no statistically significant difference between the two measurement methods for sulfate and nitrate. The large correlation coefficients (with $P < 0.01$) and P values from the rank-sum test indicate that the sulfate and nitrate concentrations from the AIM-IC and ADSS were comparable.

In 2013, a FRM sampler (Partisol $PM_{2.5}$ sampler) was collocated with the AIM-IC at AMS 7 and results from 36 pairs of samples were obtained for the intercomparison (Figure 5). The P values from Mann-Whitney rank-sum test were 0.12 for SO_4^{2-}, 0.86 for NO_3^-, and <0.001 for NH_4^+. A P value smaller than 0.001 indicates that there is a statistically significant difference between the two measurement methods. Spearman rank-order correlation coefficients were 0.95 for

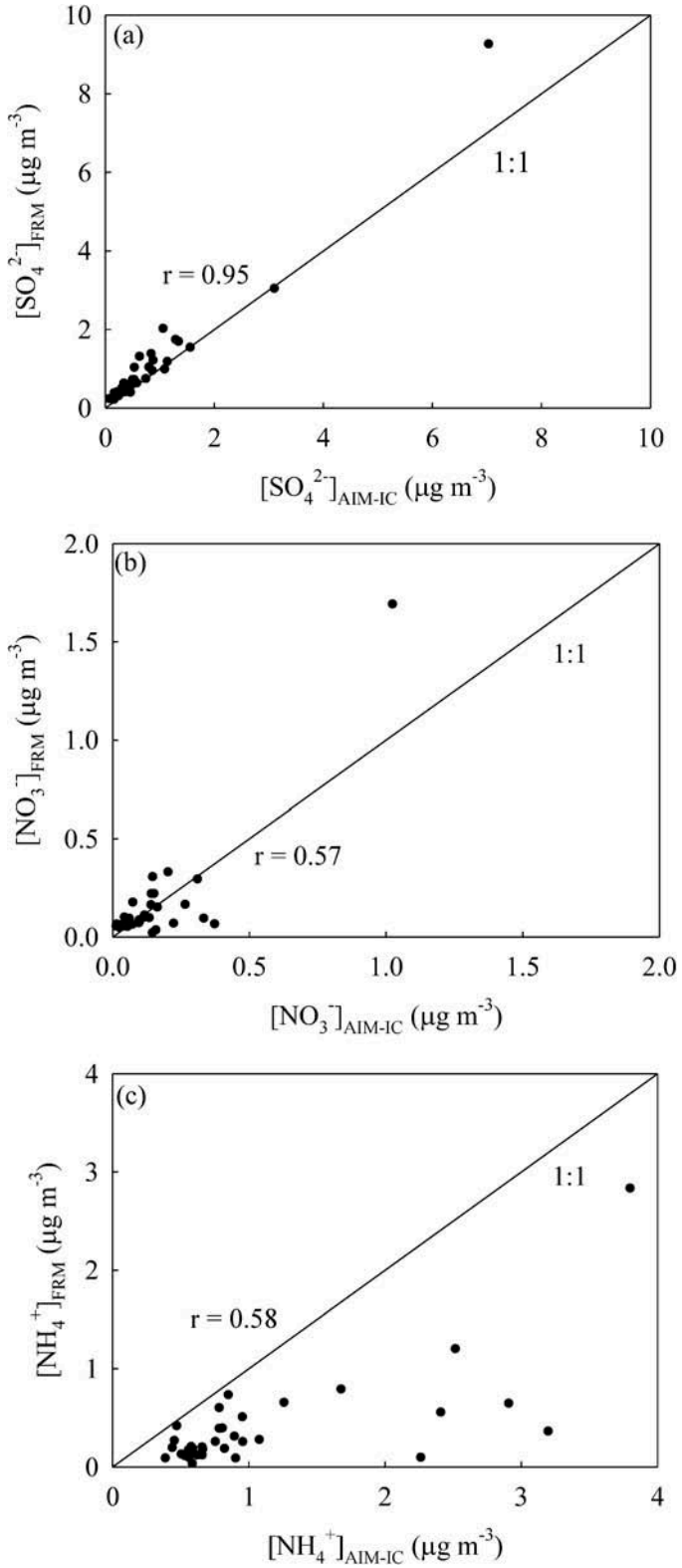

Figure 5. Intercomparison between WBEA's AIM-IC and FRM measurements of (a) sulfate, (b) nitrate, and (c) ammonium (r is the Spearman rank-order correlation coefficient) at AMS 7.

SO_4^{2-}, 0.57 for NO_3^-, and 0.58 for NH_4^+. The NH_4^+ concentrations from the AIM-IC were higher than those from the FRM, as shown in Figure 5c.

The inconsistencies in NO_3^- and NH_4^+ concentrations between the AIM-IC and FRM measurements are expected due to the differences of the two sample collection principles. It is well known that a volatilization loss in a filter-based measurement such as FRM can result in the underestimation of semivolatile compounds (e.g., NH_4^+, NO_3^-, and Cl^-) (Appel et al., 1979; Zhang and McMurry, 1992; Chow, 1995). The AIM-IC is not prone to the volatilization loss problems found in the filter-based measurements due to its semicontinuous nature. Given the FRM method biases for NO_3^- and NH_4^+ and the good agreement between the AIM-IC and the two analytical methods in sulfate measurements (r = 0.98 for ADSS and 0.95 for FRM), it was concluded that the WBEA's AIM-IC was accurate and was capable of field deployment.

Ambient NH_3 and NH_4^+ concentrations

Monthly concentrations of NH_3 and NH_4^+ at AMS 7, from April to December of 2013, are illustrated in Figure 6. The median concentrations of NH_3 showed a seasonal cycle with a late spring/summertime maximum and wintertime minimum, ranging from 2.3 μg m^{-3} in June to 0.60 μg m^{-3} in December. The particulate-phase NH_4^+ median concentrations also showed a seasonal dependency: minimum value in September (0.52 μg m^{-3}) and maximum value in April (1.8 μg m^{-3}). The monthly median NH_4^+ concentrations were lower in the summer months from June to September. Temperature is a major factor controlling gas-phase NH_3 and particulate-phase NH_4^+ partitioning (Seinfeld and Pandis, 2006). In April, hourly NH_4^+ concentration varied significantly (from 0.2 to 11 μg m^{-3}). Few NH_4^+ peak concentrations were observed, and both SO_4^{2-} and SO_2 concentrations increased at the same time. It is possible that direct SO_2 emission from stacks resulted in elevated concentrations of NH_4^+, SO_4^{2-}, and SO_2, which will be explained in next section.

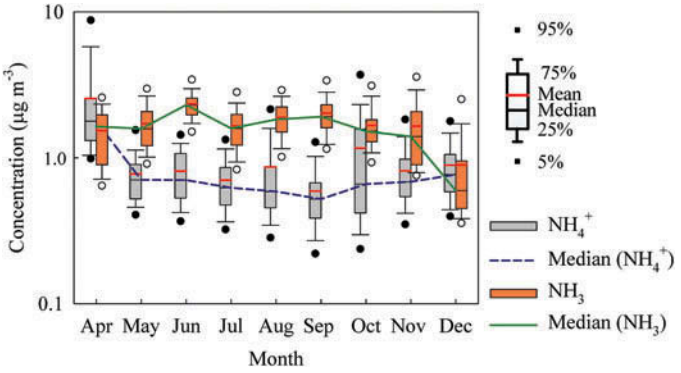

Figure 6. 2013 monthly mean and median concentrations (μg m^{-3}) of NH_3 and NH_4^+ at AMS 7. Filled circles indicate the 95th and 5th percentiles for NH_4^+ and open circles for NH_3. The total sample hours were 370, 520, 553, 690, 566, 586, 632, 606, and 737 for NH_3 and 335, 560, 554, 724, 567, 591, 639, 618, and 737 for NH_4^+ in April, May, June, July, August, September, October, November, and December, respectively.

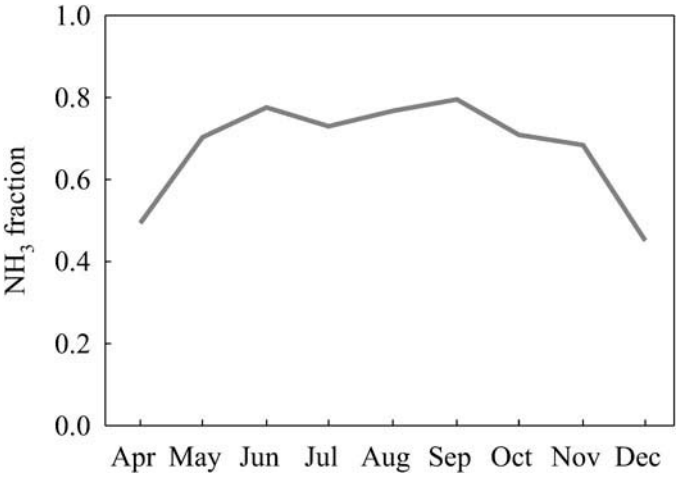

Figure 7. NH_3 gas fraction from April to December 2013 at AMS 7. The NH_3 gas fraction is defined as $[NH_3]/([NH_3]+[NH_4^+])$, molar fraction.

The NH_3 gas molar fraction ($[NH_3]/([NH_3]+[NH_4^+])$) increased with temperature (Figure 7), reaching 0.8 in the summer and decreasing to 0.45 in the winter. In the AOSR, the temperature can be as low as −40 °C in the winter months and as high as 35 °C in summer. The NH_3 gas fraction increased as ambient temperature increased and decreased as temperature decreased. With the higher concentration of gas-phase NH_3 and the greater deposition velocity in summer, the higher dry deposition of ($[NH_3]$ + $[NH_4^+]$) as N could be expected in the AOSR.

Globally, the major emission sources of NH_3 are (1) agricultural (domestic animals, synthetic fertilizers, crops): 37.4 Tg N yr^{-1}; (2) natural (oceans, undisturbed soils, wild animals): 10.7 Tg N yr^{-1}; (3) biomass burning: 6.4 Tg N yr^{-1}; and (4) other (humans and pets, industrial processes, fossil fuels): 3.1 Tg N yr^{-1} (Bouwman et al., 1997). In the AOSR, however, NH_3 mainly originates from natural sources and oil sands operations activities. Its residence time in the ambient air ranges from hours to a few days and wet and dry deposition of NH_3 are the main atmospheric removal mechanisms (Moller and Schieferdecker, 1985; Erisman et al., 1988; Seinfeld and Pandis, 2006). Ambient NH_3 concentrations vary significantly (Table 1). In the remote areas, the NH_3 concentration can be as low as 3 μg m^{-3}, whereas close to emission sources, the concentrations could reach 30 μg m^{-3} in summer in agricultural regions (Day et al., 2012). The NH_3 mean concentration in summer months at AMS 7 was 1.9 μg m^{-3}, close to or slightly lower than the concentration measured in the Canadian urban centers Edmonton, Toronto, and Montreal and at a Colorado grassland, but higher than what was found in Helsinki, Finland, a metropolitan area with little heavy industrial activity or agriculture (Table 1).

Ambient SO_2 and SO_4^{2-} concentrations

Annual average SO_2 concentrations monitored in Canada ranged from 2.1 μg m^{-3} in Atlantic Canada to 7.7 μg m^{-3} in southern Ontario (Table 1). The mean SO_2 concentration at AMS 7 was 1.4 μg m^{-3}, lower than that in Atlantic Canada, southern Quebec, southern Ontario, and British Columbia.

Table 1. Ambient NH_3, SO_2, and HNO_3 concentration (μg m^{-3})

Sampling Site	NH_3	SO_2	HNO_3	Method	Reference
Helsinki, Finland (winter)	0.01		0.24	MARGA	Makkonen et al. (2012)
Helsinki, Finland (spring)	0.1		0.4		
Singapore	3.24	4.52	0.7	MARGA	Khezri et al. (2013)
Rocky Mountain National Park	0.5			ADSS	Beem et al. (2010)
Rural grasslands (summer)[a]	3			ADSS and Radiello passive sampler	Day et al. (2012)
Suburban-urban sites (summer)[a]	4–11				
Intensive livestock feeding and farming operations (summer)[a]	30				
Edmonton, AB (winter)	2.1			Honeycomb glass denuder sampling system	Dabek-Zlotorzynska et al. (2011)
Edmonton, AB (summer)	2				
Toronto, ON (winter)	0.7				
Toronto, ON (summer)	3.1				
Montreal, QC (winter)	0.7				
Montreal, QC (summer)	2.8				
Halifax, NS (winter)	0.1				
Halifax, NS (summer)	0.8				
Atlantic Canada[b]		2.1		FEM SO_2 monitor	Environment Canada[c]
Southern Quebec[b]		4.5			
Southern Ontario[b]		7.7			
Prairies and northern Ontario[b]		2.4			
British Columbia[b]		4.52			
Saturna, BC			0.795	Filter pack	Zbieranowski and Aherne (2011)
Experimental Lakes area, ON			0.293		
Algoma, ON			0.703		
Longwoods, ON			1.186		
Egbert, ON			1.163		
Chalk River, ON			0.496		
Chapais, QC			0.156		
Fort McMurray—summer[d]	1.9	1.35	0.24	AIM-IC	This study
Fort McMurray—winter[e]	1.3	1.35	0.1		
Fort McMurray—annual[f]	1.7	1.35	0.19		

Notes: [a]Northeastern Colorado. [b]2011. [c]http://www.ec.gc.ca. [d]From May to October 2013. [e]April, November, and December in 2013. [f]From April to December 2013.

Sulfur dioxide is a primary pollutant and is emitted from anthropogenic emission sources. The major emission source is the oil sands operation in the AOSR. Sulfur dioxide is the precursor gas of particulate SO_4^{2-} and can undergo oxidation with OH in the gas phase or heterogeneously with hydrogen peroxide to form particulate sulfuric acid. Atmospheric ammonia can react to neutralize sulfuric acid and form particulate salts containing NH_4^+ and SO_4^{2-} (Seinfeld and Pandis, 2006). The monthly concentrations for both SO_2 and $PM_{2.5}$ SO_4^{2-} for AMS 7 are shown in Figure 8.

Sulfate and NH_4^+ were the most abundant inorganic ions in the region. On April 3, July 21, and August 26, 2013, elevated SO_2 concentrations (maxima = 21, 37, 46 μg m^{-3} and the corresponding wind direction = 358°, 352°, and 345°) were reported due to direct stack emissions ~35 km away from the sampling site during facility maintenance. Measurements show that both SO_4^{2-} and NH_4^+ concentrations increased as SO_2 concentration increased on April 3 and July 21, 2013 (Figure 9), to 37 μg m^{-3}. On August 26, elevated concentrations of SO_2, SO_4^{2-} and NH_4^+ were also measured, with the maximum concentrations of SO_4^{2-} and NH_4^+ at 28 and 10 μg m^{-3}, respectively. The SO_2 emitting from the stack could be oxidized and react with NH_3 to form $(NH_4)_2SO_4$ and/or NH_4HSO_4, resulting in elevated $PM_{2.5}$ sulfate and ammonium concentrations.

Aerosol neutralization ratio (ANR), the normality (or equivalent concentration) ratio of base (NH_4^+) to acids (SO_4^{2-} and NO_3^-), or $[NH_4^+]/(2 \times [SO_4^{2-}] + [NO_3^-])$, decreased as SO_2 concentrations increased. The minimum ANR during the period was 0.55, indicating that the particles were acidic and not yet fully neutralized by NH_3. Nitrate concentration increased slightly during the event, but SO_4^{2-} was the major acidic species. The Spearman rank-order correlation coefficient between SO_4^{2-} and NH_4^+ was 0.73, suggesting that the $(NH_4)_2SO_4$ and/or NH_4HSO_4 dominated the fine aerosol mode. It is likely that the particulate-phase SO_4^{2-} and NH_4^+ were formed during the transport from the stacks to the sampling

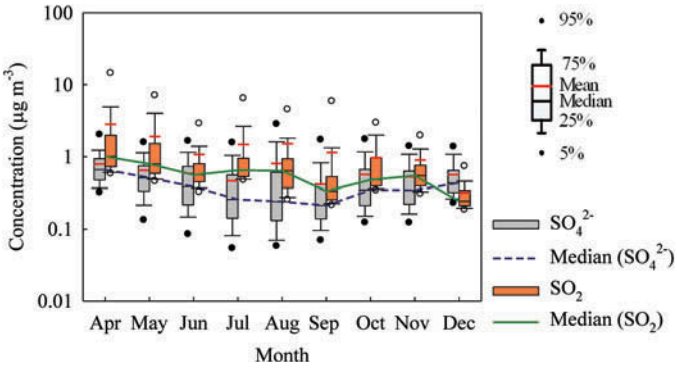

Figure 8. 2013 monthly mean and median concentrations (μg m^{-3}) of SO_2 and SO_4^{2-} at AMS 7. Filled circles indicate the 95th and 5th percentiles for SO_4^{2-} and open circles for SO_2. The total sample hours were 370, 535, 553, 690, 562, 590, 631, 606, and 737 for SO_2 and 346, 560, 553, 724, 560, 591, 633, 618, and 737 for SO_4^{2-} in April, May, June, July, August, September, October, November, and December, respectively.

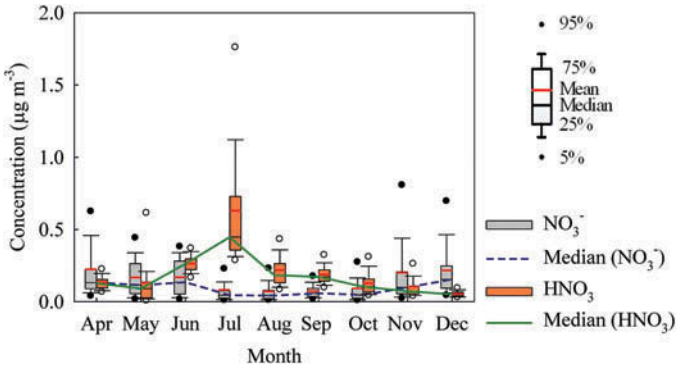

Figure 10. 2013 monthly mean and median concentrations (μg m^{-3}) of HNO_3 and NO_3^- at AMS 7. Filled circles indicate the 95th and 5th percentiles for NO_3^- and open circles for HNO_3. The total sample hours were 370, 545, 553, 629, 562, 586, 631, 606, and 737 for HNO_3 and 346, 560, 554, 724, 567, 591, 637, 618, and 736 for NO_3^- in April, May, June, July, August, September, October, November, and December, respectively.

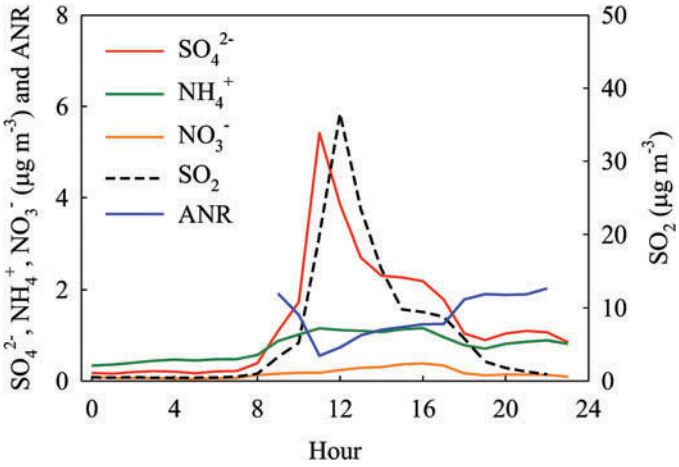

Figure 9. Hourly concentrations of SO_4^{2-}, NH_4^+, and SO_2 on July 21, 2013, at AMS 7. Aerosol neutralization ratio (ANR) is the mole equivalent concentration ratio of base (NH_4^+) to acids (SO_4^{2-} and NO_3^-).

site. The same relation was observed in December of 2013 when SO_2 concentrations were lower. This further indicates that emission and oxidation of SO_2 significantly influence particulate-phase SO_4^{2-} and NH_4^+ concentration in the AOSR and that this influence is independent of the time of year.

Ambient HNO_3 and NO_3^- concentrations

The monthly HNO_3 concentrations from May to October (summer) were higher than in the winter months (0.43 μg m^{-3} in July and 0.05 μg m^{-3} in December), and NO_3^- concentration was lower in the summer (0.04 μg m^{-3} in July and August) (Figure 10). HNO_3 concentrations measured from other studies were compared with our AOSR data (Table 1). Our values (0.19 μg m^{-3} from April to December 2013) are relatively low compared with many Canadian sites measured by the Canadian Air and Precipitation Monitoring Network (CAPMoN) network and are roughly similar to Helsinki's. Nitric acid is a secondary pollutant, and the removal mechanisms are dry deposition, wet deposition, and the interaction with aerosols. The HNO_3 formation mechanism was described by Seinfeld and Pandis (2006). The production rate of HNO_3 is a function of the concentrations of hydroxyl radical, [OH], and nitrogen dioxide, [NO_2]. With higher OH concentration during the daytime, the HNO_3 formation should be more active in summer months. In winter months, the NO_2 concentrations were usually higher in the AOSR due to low vertical mixing caused by a shallow planetary boundary layer (PBL). Elevated NO_2 concentration should favor HNO_3 formation, but this was not observed in the winter months in the AOSR. It is likely that the conditions (e.g., low OH concentration) did not favor HNO_3 formation.

To investigate the photochemistry of nitrogen species (or HNO_3 formation rate) in the AOSR, diurnal variations of HNO_3, NO_2, as well as O_3 concentrations and GSR were measured in June, August, October, and December 2013 at AMS 7 (Figure 11). The maximum peak GSR reached 366 W m^{-2} at noon in June and the minimum peak GSR was 21.8 W m^{-2} at 1:00 p.m. in December. In June and August, O_3 concentrations showed a typical diurnal pattern, with minimum values in the early morning during rush hour as a result of the reaction of O_3 with NO from traffic to form NO_2. With the increase in solar radiation during the day, more O_3 was formed, whereas in the afternoon, the NO from the evening traffic titrated the O_3. The maximum hourly O_3 concentration was 33 ppb at 4:00 p.m. in June and 30 ppb at 4:00 p.m. in August.

The obvious O_3 diurnal variation that was observed in June and August became less clear in December, indicating less active photochemical reactions in winter with low temperature and low GSR (Pudasainee et al., 2006). For HNO_3, the diurnal patterns showed higher concentration during the daytime in the summer, with a maximum HNO_3 concentration of 0.31 μg m^{-3} at 10:00 a.m. in June and 0.28 μg m^{-3} at 11:00 a.m. in August. No clear HNO_3 pattern could be identified during the December sampling period. The OH radical is an important species for the O_3 formation. The weak O_3 diurnal pattern in winter months could be potentially used as an indicator of inactive

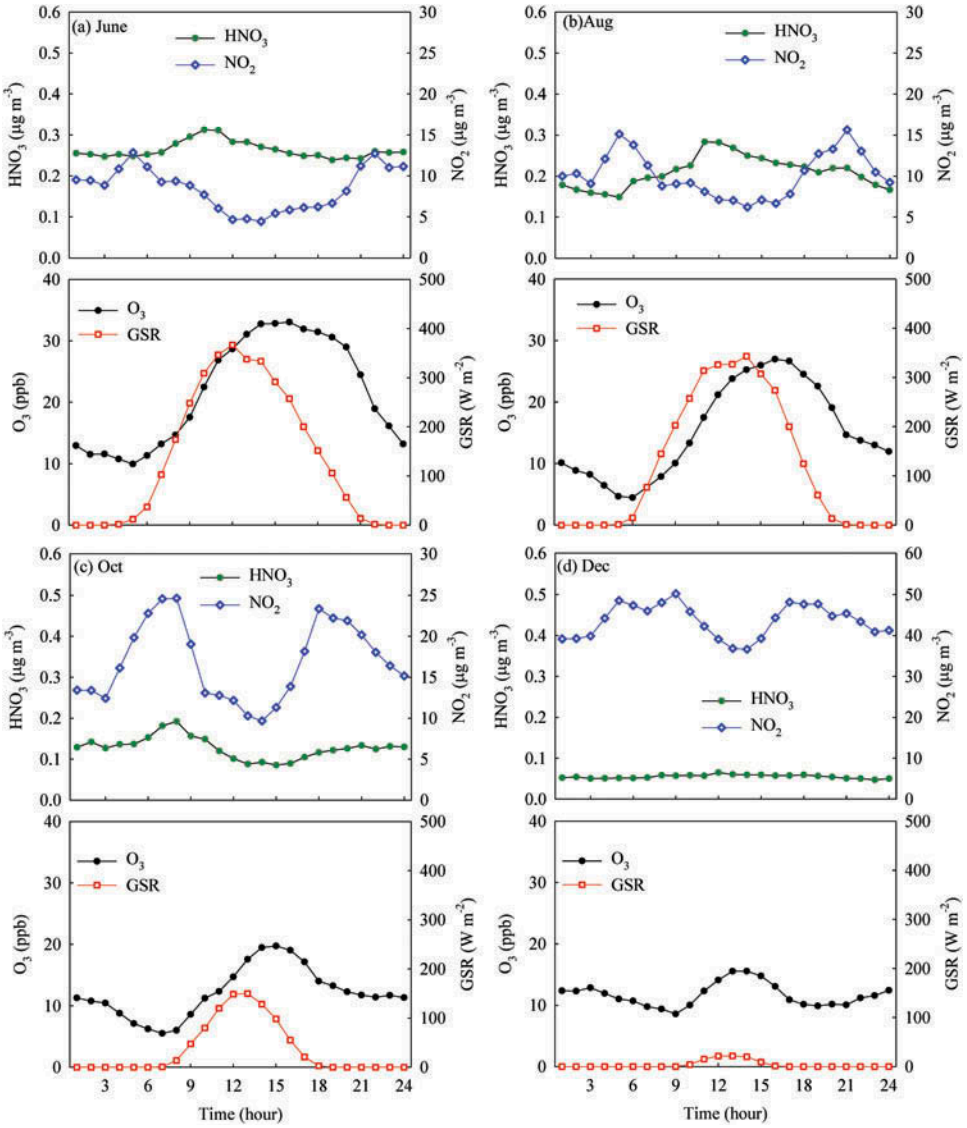

Figure 11. Diurnal profiles of HNO_3, NO_2, O_3, and GSR in (a) June, (b) August, (c) October, and (d) December of 2013 at AMS 7.

photochemistry and low OH radical concentration resulting in low HNO_3 formation in winter months. Further studies should be conducted to investigate the OH concentration level.

HNO_3 concentration in summer was higher than NO_3^- concentration, and NO_3^- concentration observed in winter was slightly higher than HNO_3 (Figure 10). The median NO_3^- concentration in December was 0.15 μg m^{-3} compared with 0.04 μg m^{-3} in the summer (July and August). The elevated nitrate concentration at this sampling site was likely related to the direct emission of diesel power generators located near the sampling site or traffic. Nitrate (NO_3^-) is the dominant particulate-phase inorganic ion from the diesel power generators and results from the high-temperature combustion of diesel fuel, which results in thermal nitrogen oxide (NO_x) formation (Chiang et al., 2012). HNO_3 prefers to form ammonium nitrate (NH_4NO_3) in particulate phase in cold temperature (Seinfeld and Pandis, 2006).

In summary, with the new CAAQS for $PM_{2.5}$ in 2015, the understanding of the chemistry of $PM_{2.5}$ SO_4^{2-}, NO_3^-, and NH_4^+ and its precursor gases is essential for developing possible $PM_{2.5}$ management strategies in the AOSR. As indicated in subsection "Ambient SO_2 and SO_4^{2-} concentrations," SO_2 emitted directly from stacks could undergo the SO_2 heterogeneous oxidation and result in elevated $PM_{2.5}$ related SO_4^{2-} and NH_4^+.

Forest fire effect on AOSR air quality

Wildfires, an important $PM_{2.5}$ source, are common in northern Canada in the summertime. In 2011, a series of forest fires burned ~10 km from AMS 1 and fire plumes were sampled several times during the fire period from May 15 to August 30 of 2011. The measured hourly concentrations of NO_3^-, NH_4^+, SO_4^{2-}, SO_2, HNO_3, NH_3, and $PM_{2.5}$ (measured by the TEOM in May and by the SHARP $PM_{2.5}$ monitor in June) in June 2011 are illustrated in Figure 12a, b, and c. All NO_3^-, NH_4^+, HNO_3, NH_3, and $PM_{2.5}$ concentrations increased during the forest fire, and the similar pattern was identified for four

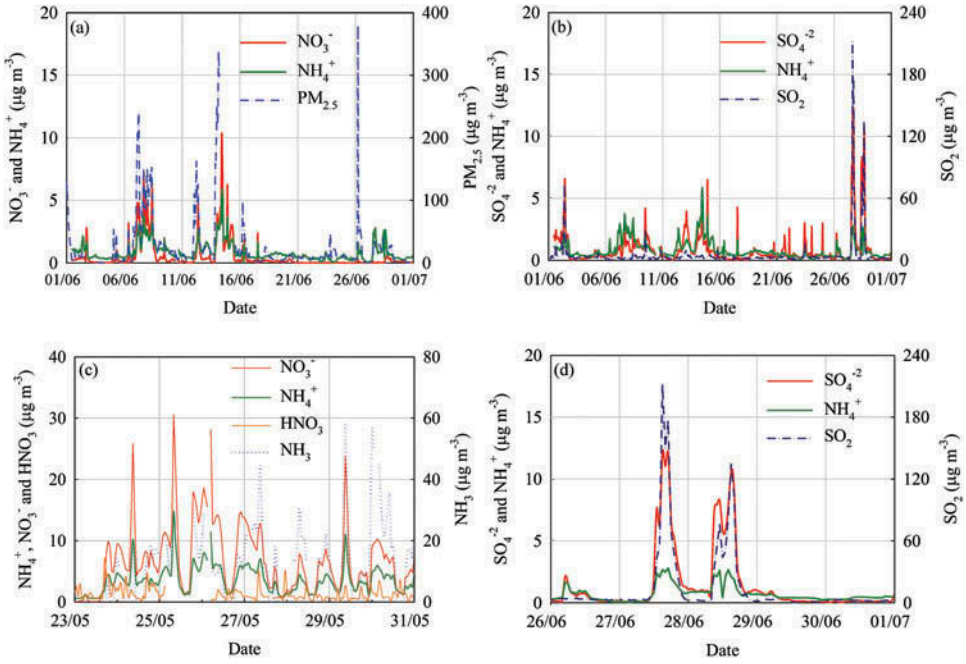

Figure 12. Hourly concentrations of NO_3^-, SO_4^{2-}, NH_4^+, SO_2, and total $PM_{2.5}$ in June of 2011 at AMS 1.

species. The maximum concentrations of NO_3^-, NH_4^+, HNO_3, and NH_3 were 31, 15, 9.6 and 89 μg m^{-3} in May. Nitrate and ammonium were the major ions and the high correlation coefficient, 0.88, suggested NH_4NO_3 formation. The maximum $PM_{2.5}$ concentration was greater than 450 μg m^{-3}, the upper limit of $PM_{2.5}$ real-time TEOM monitor. For HNO_3 gaseous- and particulate-phase partition, particulate NO_3^- was the major form. In contrast, the NH_3 concentration was significantly higher than the NH_4^+ concentration. All four species, NO_3^-, NH_4^+, HNO_3, and NH_3, are important N sources for the ecosystem. During the forest fire, the elevated concentrations of NO_3^-, NH_4^+, HNO_3, and NH_3 could result in higher N deposition to the ecosystem.

Before June 18, 2011, NH_4^+ concentrations increased as NO_3^- concentrations increased, suggesting the formation of NH_4NO_3 in the fire plume. After June 26 (Figure 12d), the NH_4^+ concentrations tended to increase when SO_4^{2-} and SO_2 concentrations increased and NO_3^- concentration remained relatively unchanged. The elevated NH_4^+ and $PM_{2.5}$ concentrations after June 26 were therefore not likely associated with forest fires and were more likely related to SO_2 emissions from stacks that resulted in the elevated concentrations of NH_4^+, SO_4^{2-}, and $PM_{2.5}$. With the characterization of $PM_{2.5}$ chemical species by the AIM-IC, the $PM_{2.5}$ source could be properly identified immediately.

Conclusion

WBEA's AIM-IC with two types of parallel-plate denuder membranes was evaluated by measuring NH_3, SO_2, and HNO_3 gas standards of known concentrations. The collection efficiencies of SO_2 and HNO_3 with the cellulose membrane were 96% and 100%, respectively, though reaching optimal capture efficiencies took longer than anticipated in laboratory calibrations. Nylon membrane filters were determined to be better for measuring NH_3 concentrations. Overall, the SO_2 concentrations from the continuous monitor and $PM_{2.5}$ sulfate concentrations from the ADSS and Partisol $PM_{2.5}$ sampler agreed well with the AIM-IC. Hence, WBEA's AIM-IC is considered a suitable method for the measurements of ambient SO_2, NH_3, HNO_3, and $PM_{2.5}$ water-soluble inorganic species.

In general, SO_2, NH_3, and HNO_3 concentrations were low by comparing with other cities in Canada. The HNO_3 (0.21 ± 0.26 μg m^{-3}) and NO_3^- (0.14 ± 0.20 μg m^{-3}) concentrations were generally low in the AOSR, even in the winter when NO_2 concentration was high. It is possible that the OH radical concentration was too low for the HNO_3 formation in the winter. Three major $PM_{2.5}$ formation mechanisms were identified. First, NH_3 concentrations in the summer were higher than those in the winter months and temperature significantly influenced the NH_3/NH_4^+ partitioning. Secondly, sulfate and ammonium were the most abundant inorganic ions in the particulate phase. Both concentrations increased significantly when SO_2 concentration increased (unstable stack SO_2 emission during facility maintenance of oil sands plants), suggesting that (1) ammonium sulfate and/or bisulfate dominated the inorganic $PM_{2.5}$ composition in the plumes, and (2) SO_2 played an important role in controlling the concentrations of both particulate-phase species. The more effective SO_2 management should be able to reduce the $PM_{2.5}$ concentration for this situation. Thirdly, the AIM-IC monitored the $PM_{2.5}$ water-soluble ionic species at AMS 1 where it was in proximity to a forest fire in the summer of 2011. High concentrations of NH_4^+, NO_3^-, HNO_3, NH_3, and $PM_{2.5}$ were observed, suggesting that ammonium nitrate dominated the $PM_{2.5}$ inorganic

composition during the forest fire period. Continued monitoring and analysis of AIM-IC is required to further constrain how local anthropogenic and nonanthropogenic sources impact the local air quality in the AOSR.

Nomenclature

ADSS	annular denuder sampling system
AIM-IC	ambient ion monitor–ion chromatograph
AMS	air monitoring station
ANR	aerosol neutralization ratio
AOSR	Athabasca Oil Sands Region
CAAQS	Canadian Ambient Air Quality Standards
CalNex	California Nexus
CAPMoN	Canadian Air and Precipitation Monitoring Network
FEM	Federal Equivalent Method
FRM	Federal Reference Method
GSR	global solar radiation
IC	ion chromatograph
MARGA	monitoring for aerosols and gases
NAPS	Canadian National Air Pollution Surveillance
$PM_{2.5}$	particulate matter with aerodynamic diameter of less than 2.5 μm
PPWD	parallel-plate wet denuder
PSSC	particle super saturation chamber
SHARP	synchronized hybrid ambient real-time particulate
TEOM	tapered element oscillating microbalance monitor
TSP	total suspended particulate
WBEA	Wood Buffalo Environmental Association

Acknowledgment

The content and opinions expressed by the authors in this study do not necessarily reflect the views of the WBEA or of the WBEA membership. The authors would like to thank A. Legge for establishing the project, and D. Spink, K. Percy, M. Markovic, and C. Watt for their valuable comments and suggestions.

References

Ahlm, L., S. Liu, D.A. Day, L.M. Russell, R. Weber, D.R. Gentner, A.H. Goldstein, J.P. DiGangi, S.B. Henry, F.N. Keutsch, T.C. VandenBoer, M.Z. Markovic, J.G. Murphy, X.R. Ren, and S. Scheller. 2012. Formation and growth of ultrafine particles from secondary sources in Bakersfield, California. *J. Geophys. Res. Atmos*. 117:D00V08. doi:10.1029/2011JD017144

Appel, B.R., S.M. Wall, Y. Tokiwa, and M. Haik. 1979. Interference effects in sampling particulate nitrate in ambient air. *Atmos. Environ*. 13:319–325. doi:10.1016/0004-6981(79)90175-6

Beem, K.B., S. Raja, F.M. Schwandner, C. Taylor, T. Lee, A.P. Sullivan, C.M. Carrico, G.R. McMeeking, D. Day, E. Levin, J. Hand, S.M. Kreidenweis, B. Schichtel, W.C. Malm, and J.L. Collett. 2010. Deposition of reactive nitrogen during the Rocky Mountain Airborne Nitrogen and Sulfur (RoMANS) study. *Environ. Pollut*. 158:862–872. doi:10.1016/j.envpol.2009.09.023

Bouwman, A.F., D.S. Lee, W.A.H. Asman, F.J. Dentener, K.W. VanderHoek, and J.G.J. Olivier. 1997. A global high-resolution emission inventory for ammonia. *Glob. Biogeochem. Cycles* 11:561–587. doi:10.1029/97gb02266

Brauer, M., P. Koutrakis, J.M. Wolfson, and J.D. Spengler. 1989. Evaluation of the gas collection of an annular denuder system under simulated atmospheric conditions. *Atmos. Environ*. 23:1981–1986. doi:10.1016/0004-6981(89)90524-6

Chiang, H.L., Y.M. Lai, and S.Y. Chang. 2012. Pollutant constituents of exhaust emitted from light-duty diesel vehicles. *Atmos. Environ*. 47: 399–406. doi:10.1016/j.atmosenv.2011.10.045

Chow, J.C. 1995. Measurement methods to determine compliance with ambient air-quality standards for suspended particles. *J. Air Waste Manage. Assoc*. 45:320–382. doi:10.1080/10473289.1995.10467369

Dabek-Zlotorzynska, E., T.F. Dann, P.K. Martinelango, V. Celo, J.R. Brook, D. Mathieu, L.Y. Ding, and C.C. Austin. 2011. Canadian National Air Pollution Surveillance (NAPS) $PM_{2.5}$ speciation program: Methodology and $PM_{2.5}$ chemical composition for the years 2003–2008. *Atmos. Environ*. 45:673–686. doi:10.1016/j.atmosenv.2010.10.024

Davies, M., R. Person, U. Nopmongcol, T. Shah, K. Vijayaraghavan, R. Morris, and D. Picard. 2012. *Lower Athabasca Region Source and Emission Inventory*. Fort McMurray, Alberta: Cumulative Environmental Management Association.

Day, D.E., X. Chen, K.A. Gebhart, C.M. Carrico, F.M. Schwandner, K.B. Benedict, B.A. Schichtel, and J.L. Collett. 2012. Spatial and temporal variability of ammonia and other inorganic aerosol species. *Atmos. Environ*. 61:490–498. doi:10.1016/j.atmosenv.2012.06.045

Du, H.H., L.D. Kong, T.T. Cheng, J.M. Chen, J.F. Du, L. Li, X.G. Xia, C.P. Leng, and G.H. Huang. 2011. Insights into summertime haze pollution events over Shanghai based on online water-soluble ionic composition of aerosols. *Atmos. Environ*. 45:5131–5137. doi:10.1016/j.atmosenv.2011.06.027

Ellis, R.A., J.G. Murphy, M.Z. Markovic, T.C. VandenBoer, P.A. Makar, J. Brook, and C. Mihele. 2011. The influence of gas-particle partitioning and surface-atmosphere exchange on ammonia during BAQS-Met. *Atmos. Chem. Phys*. 11:133–145. doi:10.5194/acp-11-133-2011

Erisman, J.W., A.W.M. Vermetten, W.A.H. Asman, A. Waijersijpelaan, and J. Slanina. 1988. Vertical-distribution of gases and aerosols—The behavior of ammonia and related components in the lower atmosphere. *Atmos. Environ*. 22:1153–1160. doi:10.1016/0004-6981(88)90345-9

Fan, J., X.Y. Yue, Y. Jing, Q. Chen, and S.G. Wang. 2014. Online monitoring of water-soluble ionic composition of PM_{10} during early summer over Lanzhou City. *J. Environ. Sci. China* 26:353–361. doi:10.1016/S1001-0742(13)60431-3

Febo, A., C. Perrino, and M. Cortiello. 1993. A denuder technique for the measurement of nitrous acid in urban atmospheres. *Atmos. Environ. A* 27:1721–1728. doi:10.1016/0960-1686(93)90235-Q

Ferm, M., and A. Sjodin. 1985. A sodium-carbonate coated denuder for determination of nitrous acid in the atmosphere. *Atmos. Environ*. 19: 979–983. doi:10.1016/0004-6981(85)90243-4

Gao, X.M., L.X. Yang, S.H. Cheng, R. Gao, Y. Zhou, L.K. Xue, Y.P. Shou, J. Wang, X.F. Wang, W. Nie, P.J. Xu, and W.X. Wang. 2011. Semi-continuous measurement of water-soluble ions in $PM_{2.5}$ in Jinan, China: Temporal variations and source apportionments. *Atmos. Environ*. 45:6048–6056. doi:10.1016/j.atmosenv.2011.07.041

Gosselin, P., S. Hrudey, M.A. Naeth, A. Plourde, R. Therrien, G. van Der Kraak, and Z. Xu. 2010. *Environmental and Health Impacts of Canada's Oil Sands Industry*, 404. Ottawa, Canada: Royal Society of Canada.

Harrison, R.M., and A.M.N. Kitto. 1990. Field intercomparison of filter pack and denuder sampling methods for reactive gaseous and particulate pollutants. *Atmos. Environ. A* 24:2633–2640. doi:10.1016/0960-1686(90)90142-A

Khezri, B., H. Mo, Z. Yan, S.L. Chong, A.K. Heng, and R.D. Webster. 2013. Simultaneous online monitoring of inorganic compounds in aerosols and gases in an industrialized area. *Atmos. Environ*. 80:352–360. doi:10.1016/j.atmosenv.2013.08.008

Makkonen, U., A. Virkkula, J. Mantykentta, H. Hakola, P. Keronen, V. Vakkari, and P.P. Aalto. 2012. Semi-continuous gas and inorganic aerosol

measurements at a Finnish urban site: Comparisons with filters, nitrogen in aerosol and gas phases, and aerosol acidity. *Atmos. Chem. Phys*. 12:5617–5631. doi:10.5194/acp-12-5617-2012

Markovic, M.Z., T.C. VandenBoer, and J.G. Murphy. 2012. Characterization and optimization of an online system for the simultaneous measurement of atmospheric water-soluble constituents in the gas and particle phases. *J. Environ. Monit*. 14:1872–1884. doi:10.1039/c2em00004k

Moller, D., and H. Schieferdecker. 1985. A relationship between agricultural NH_3 emissions and the atmospheric SO_2 content over industrial-areas. *Atmos. Environ*. 19:695–700. doi:10.1016/0004-6981(85)90056-3

Nie, W., T. Wang, X.M. Gao, R.K. Pathak, X.F. Wang, R. Gao, Q.Z. Zhang, L.X. Yang, and W.X. Wang. 2010. Comparison among filter-based, impactor-based and continuous techniques for measuring atmospheric fine sulfate and nitrate. *Atmos. Environ*. 44:4396–4403. doi:10.1016/j.atmosenv.2010.07.047

Percy, K.E. 2013. Ambient air quality and linkage to ecosystems in the Athabasca Oil Sands, Alberta. *Geosci. Canada* 40:182–201.

Pudasainee, D., B. Sapkota, M.L. Shrestha, A. Kaga, A. Kondo, and Y. Inoue. 2006. Ground level ozone concentrations and its association with NO_x and meteorological parameters in Kathmandu Valley, Nepal. *Atmos. Environ*. 40:8081–8087. doi:10.1016/j.atmosenv.2006.07.011

Seinfeld, J.H., and S.N. Pandis. 2006. *Atmospheric Chemistry and Physics: From Air Pollution to Climate Change*, 2nd ed. New York: Wiley.

Stringham, G. 2012. Energy developments in Canada's oil sands. In *Alberta Oil Sands Energy, Industry and the Environment*, ed. K. E. Percy, 19–34. Oxford, UK: Elsevier.

Sudheer, A.K., R. Rengarajan, D. Deka, R. Bhushan, S.K. Singh, and M.Y. Aslam. 2014. Diurnal and seasonal characteristics of aerosol ionic constituents over an urban location in western India: Secondary aerosol formation and meteorological influence. *Aerosol Air Qual. Res*. 14:1701–1713. doi:10.4209/aaqr.2013.09.0288

Upadhyay, S., K. Ganguly, and T. Stoeger. 2014. Inhaled ambient particulate matter and lung health burden. *Eur. Med. J. Respir*. 2:88–95.

Wu, W.S., and T. Wang. 2007. On the performance of a semi-continuous $PM_{2.5}$ sulphate and nitrate instrument under high loadings of particulate and sulphur dioxide. *Atmos. Environ*. 41:5442–5451. doi:10.1016/j.atmosenv.2007.02.025

Zbieranowski, A.L., and J. Aherne. 2011. Long-term trends in atmospheric reactive nitrogen across Canada: 1988–2007. *Atmos. Environ*. 45:5853–5862. doi:10.1016/j.atmosenv.2011.06.080

Zhang, X.Q., and P.H. McMurry. 1992. Evaporative losses of fine particulate nitrates during sampling. *Atmos. Environ. A* 26:3305–3312. doi:10.1016/0960-1686(92)90347-N

About the Authors

Yu-Mei Hsu is an atmospheric and analytic chemist, and **Thomas A. Clair** is a lead scientist for Wood Buffalo Environmental Association in Fort McMurray, Alberta, Canada.